Munich Personal RePEc Archive

Climate change: where is the hockey stick? evidence from millennial-scale reconstructed and updated temperature time series.

Travaglini, Guido

Università di Roma "La Sapienza"

25 December 2011

Online at https://mpra.ub.uni-muenchen.de/35565/
MPRA Paper No. 35565, posted 25 Dec 2011 21:57 UTC

Climate Change: Where is the Hockey Stick? Evidence from Millennial-Scale Reconstructed and Updated Temperature Time Series.

Guido Travaglini
Istituto di Economia e Finanza
Università di Roma "La Sapienza"
Email: jay_of_may@yahoo.com
December, 2011.

Keywords: Hockey Stick Controversy, Time Series, Kalman Filter.
JEL Classification: C22: Time-Series Models; C51: Model Construction and Estimation; Q54: Climate, Natural Disasters, Global Warming.

Abstract

The goal of this paper is to test on a millennial scale the magnitude of the recent warmth period, known as the "hockey-stick", and the relevance of the causative anthropogenic climate change hypothesis advanced by several academics and worldwide institutions. A select batch of ten long-term climate proxies, included in the NOAA 92 PCN dataset all of which running well into the nineties, is updated to the year 2011 by means of a Time-Varying Parameter Kalman Filter SISO model for state prediction. This procedure is applied by appropriately selecting as observable one out of the HADSST2 and of the HADCRUT3 series of instrumental temperature anomalies available since the year 1850. The updated proxy series are thereafter individually tested for the values and time location of their four maximum non-neighboring attained temperatures. The results are at best inconclusive, since three of the updated series, including Michael Mann's celebrated and controversial tree-ring reconstructions, do not refute the hypothesis, while the others quite significantly point to different dates of maximum temperature achievements into the past centuries, in particular those associated to the Medieval Warm Period.

1. Introduction

More than a decade ago some climatologists, after performing past temperature reconstructions on a millennial scale, have come up with the conclusion that the recent warming period (RWP) is an unprecedented phenomenon in the climatic history of planet Earth (Mann et al., 1998, 1999). The unusual behavior exhibited by temperatures in the late 20th century was attributed by the authors to anthropogenic influences, and chiefly to the increases in recorded greenhouse gas concentrations caused by the worldwide expansion of industrial and commercial activities.

The statistical evidence produced by the authors is graphically shaped as the well renowned "hockey stick" that has been prominently featured in the Intergovernmental Panel on Climate Change (IPCC) activity since the Third Assessment Report (IPCC, 2001). Hence on, a worldwide dispute has emerged on both the validity of the empirical evidence and on its causes, thereby actively involving popular media, scientists, corporations, governments and political organizations. By consequence, the purported dramatic rise of recent temperatures and the associated anthropogenic origin have found advocates and skeptics still to date igniting the "hockey-stick curve" controversy (Montford, 2010), culminated in the "Climategate" and "Amazongate" affairs, and in the Wegman Report (2006).

Criticism of the anthropogenic origins of global warming includes studies questioning the methodology utilized for the temperature reconstructions (e.g. Baliunas and Soon, 2003; McIntyre and McKitrick, 2005, 2009), and other studies pointing to the prevalence of long-run evolving natural causes such as solar activity (Abdussamatov, 2004; Alanko-Huotari et al., 2006; Fouka et al., 2006), cosmic rays (Shaviv, 2005; Svensmark and Frijs-Christensen, 2007; Bard and Frank, 2006, Usoskin et al., 2004a, 2004b, 2006), ocean currents (Gray et al., 1997; Trouet et al., 2009), and volcanic activity (Shindell et al., 2004).

In this context, probably the only consensus among the opposing sides is couched in terms of the available evidence of climate changes on a millennial scale that may inform on the role of anthropogenic forcing in the RWP (e.g. Folland et al. 2001). In fact, the lack of widespread instrumental surface temperature estimates prior to the mid-19th century (Jones et al., 2001) has placed particular emphasis on the need to track the history of climate changes accurately, which can be achieved by utilizing carefully reconstructed long-term empirical evidence (von Storch et al., 2004; Rutherford et al., 2005; Mann et al., 2008, 2009a).

Such evidence consists of proxy data which may afford scientists with clues from the past climate changes to be compared with more recent instrumental data observations in order to enable statistical inferences on millennial-scale anomalies, such as the Medieval Warming Period (MWP) and the RWP. Many regional or global sea and/or surface temperature reconstructions have been available, customarily utilizing proxies of climate variability derived from the environment itself and from documentary evidence (Crowley and North 1991; Bradley 1999; Jones et al. 2001). Particularly useful are found to be the high-resolution proxies such as tree rings (e.g., Fritts et al. 1971; Fritts 1991; Briffa et al. 1994, 2001, 2003), corals (e.g., Evans et al. 2002; Hendy et al. 2002), ice cores (O'Brien et al. 1995; Appenzeller et al. 1998), and lake sediments (Hughen et al. 2000).

More recently, following the suggestions of a National Research Council (NRC) report (NRC, 2006) and of the IPCC Fourth Assessment Report (IPCC, 2007)[1], several scientists under the

[1] The IPCC acknowledged in the Fourth Assessment Report (2007) that the MWP was: "the warmest period prior to the 20th century very likely occurred between 950 and 1100….[however] only very large-scale climate averages can be expected to reflect global forcings over recent millennia…..[so that], in order to reduce the uncertainty, further work is necessary to update existing records, many of which were assembled up to 20 years ago, and to produce many more, especially early, paleoclimate series with much wider geographic coverage".

auspices of the National Oceanic and Atmospheric Administration (NOAA) Paleoclimatology Program have gathered in an organic and easily accessible manner a large set of studies producing reconstructed proxy data on surface and sea temperatures at hemispheric, regional and global scales for much of the last 2,000 years (Wahl et al., 2010). The proxy data are contained in the NOAA Paleoclimate Network including 92 high-resolution temperature reconstructions and proxy/instrumental data available online (http://www.ncdc.noaa.gov/paleo/recons.html).

Of these proxy data (henceforth denoted as NOAA), the longest time series with nonempty-cell observations [2] are selected in the present paper for testing on a millennial scale the issues raised in the "hockey stick" controversy and the relevance of the MWP. Details and sources of the full dataset are contained in the Data Appendix. Most series are longer than one millennium but all of them end well before the year 2011 and thus require updating by means of instrumental variables. The Best Estimated Anomaly (BEA) of the updated HADSST2 (Rayner et al., 2006) and HADCRUT3 (Brohan et al., 2006) global averages and Northern Hemisphere data are the appropriate candidates for playing this role, as their availability strides the period 1850-2011 and can be utilized for updating the proxy data by means of Kalman filtering (Kalman, 1960). All of the BEA data series are downoadable from the web at the same site as above, and include also Southern Hemisphere records, which we chose not to employ for updating purposes because of their relatively low reliability[3]. By consequence, the BEA series selected for usage amount to six out of the nine available.

Sect. 2 introduces both the selected BEA and NOAA series by displaying their timelines and their major characteristics such as descriptive and stationarity test statistics. Sect. 3 tackles the updating properties of the Time-Varying Parameter (TVP) Kalman Filter (KF) SISO model for state prediction. Sect. 4 produces the updated NOAA series, their characteristics and especially the dates associated to the maximum achieved proxy-measured temperatures. Sect. 5 concludes.

2. The selected BEA and NOAA datasets

The time-series performances of the six selected BEA series are depicted in Fig. 1 and their major statistical features are shown in Table 1. The suffix NH and GL respectively refers to data records collected in the Northern Hemisphere and globally. Both analytically and graphically, the series show no significant differences one another. In fact, means and standard deviations are not sizably different (cols. 1-2) and all of the series exhibit level nonstationarity within a marginal significance (*p*-value) of 10% of the Augmented Dickey Fuller (ADF) *t*-test statistic for unit root (Dickey and Fuller, 1979), as well as full stationarity for the corresponding first differences (cols. 5-8)[4]. Finally, the BEA series share similar minimum and maximum level dates, the former (latter) striding the 19th and the 20th (the 20th and the 21st) centuries.

---

[2] Many more NOAA series straddle the MWP but for certain years the observations are unavailable. In order to avoid arbitrary interpolation procedures, they must misfortunately be excluded from the sample presented. Among these, the millennial-scale series introduced by Loso (2008) with interesting inferences about the MWP.

[3] The Climatic Research Unit that is responsible for handling the data admittedly declares that: "Over land regions of the world over 3000 monthly station temperature time series are used [as the basic raw data]. Coverage is denser over the more populated parts of the world, particularly, the United States, southern Canada, Europe and Japan. Coverage is sparsest over the interior of the South American and African continents and over the Antarctic".

[4] The z-tests for mean inequality of the series, given the observed standard deviations (Table 1, cols. 1-2), produces the following *p*-values: 0.925, 0.9338, 0.926, 0.927, 0.925, and 0.902, all of which reject the null of no equality below the

The ten selected NOAA series are long enough to include the MWP (~900-1350 AD), and in some cases also previous likely warmings, to be compared with the RWP (Crowley and Lowery, 2000; Bradley et al., 2001; Baliunas and Soon, 2003; Loso, 2008; Esper and Frank, 2009; Trouet et al., 2009; Graham et al., 2010). The series obviously include for comparative purposes the Maunder Minimum, also known as the Little Ice Age (LIA) that has occurred in Europe (~1645-1715 AD) as a relevant event of the climatic cyclical pattern recognized by several authors (Baliunas and Soon, 2003; Bürger, 2007). By symmetry, the longest series may as well include more ancient unrecorded coolings and warmings.

Table 2, whose keynames and sources are expounded in the Data Appendix, reports important length features of the NOAA series. Most of these end in the late nineties (col. 5) and some require a substantial amount of updation steps (*s*) to fill in affordable values until the year 2011 via the proposed updation procedure (col. 8). Unreported test statistics for normality (Jarque-Bera and KPSS) indicate that none of the series is normally distributed.

Table 3 supplies major descriptive statistics and ADF test statistics for unit root of the NOAA series. Means and standard deviations (cols. 3-4) sizably differ among them and so does the volatility index (col. 5) measured as the absolute ratio of the former to the latter. Finally, the ADF test statistics and their *p*-values indicate that only four series are stationary within the 5% significance level: Hant, Mann1, D'Arrigo and Moberg.

Cointegration is important for testing the trustworthiness of the instrumental variable(s) as a predictor of the NOAA series. Lack of any common trend among the two is likely to determine biased forecasts once the variables implied were significantly orthogonal one another. Table 4 reports the Engle-Granger t-statistic and the Johansen trace test statistic (Engle and Granger, 1987; Johansen, 1988, 1991) of the NOAA with a randomly selected BEA series in the interval comprised between 1850 and the AD yearends. Because there are six available BEA series and the cointegration tests with the NOAA series are almost all identical, the BEA series selected is HADCRUT3NH, namely, the temperature anomaly records collected in the Northern Hemisphere, which is possibly the most consistent with the provenance of the original dataset.

The first test statistic, denoted as EG (cols. 3-4), is large enough in absolute terms to reject the null o no cointegration with BEA at the 1% marginal significance level for all series but Moberg, whose marginal significance is somewhere lower than 10%. The second test statistic, denoted as JO (cols. 5-6), essentially reinforces the previous results by producing enough high test statistics that are unable to reject both implied null hypotheses except for Crow[5].

In Fig. 2, panes *a* and *b* show the entire NOAA series since their beginning and including the updations to year 2011 performed in Sect. 4. The left-hand side of each figure separated by a vertical bar shows the original series and simple eyeballing may suggest that the updated observations constitute a mere blip as compared to their millennial-scale length. However, these blips may be relevant enough – at least – to test if the warming appears to have accelerated towards the present day.

10% significance level. The ADF test for unit root of the series is performed with lags of the first differences optimally selected by the Bayesian Information Criterion (BIC).

[5] The null hypothesis in JO assumes intercepts and linear trends in the cointegrating relations and quadratic trends in the data. Moreover, one lag is assumed in the underlying Vector Error Correction model. The *p*-values of the two JO test statistics are unreported for ease of space, and they hover below 1% except for the series Crow (line 6, col. 9),

3. The Time-Varying Parameter Kalman Filter SISO model for state prediction

3.1. Description of the method

The TVP-KF model for state prediction is a combination of the standard KF Linear Time Invariant (LTI) model and of the Time-Varying KF (e.g. Hamilton, 1994; Grimble, 2006). Kalman described the KF as a series of recursive linear equations in a continuous or in a discrete-time context addressed at predicting position and time of a moving target by progressively increasing accuracy of the filter's prediction at each position coordinate. The KF has enjoyed many applications in physics, engineering and in other scientific fields, and also in applied statistics (Aoki, 1990; Anderson and Moore, 2005).

Standard KF modeling (both LTI and TVP) requires utilizing the state variables ("states") and the measurable or observable variables ("observables") (Aoki, 1990; Anderson and Moore, 2005). In the present context, each of the NOAA series is treated as a state, while any of the six available BEA series is the observable, namely, the instrumental variable. In the field of statistical applications, the KF has received much attention as a forecasting procedure of the state(s) and of the observable(s), usually in competition with other methods such as Autoregressive Moving Average (ARMA), Vector Autoregression (VAR), Bayesian VAR (BVAR), Vector Error Correction Method (VECM) and Generalized Autoregressive Conditional Heteroskedasticity (GARCH). The KF is shown to outsmart GARCH (Choudry and Wu, 2008) but too little is produced in the literature to comparatively evaluate its efficiency with respect to the other methods.

TVP-KF is a tracking method that is expected to improve the accuracy of the state prediction by providing the operator with ongoing information about the timely magnitudes of the parameters involved. In order to avoid stepwise explosive behaviour of the state sequence, it may contain a self-correcting mechanism addressed at further stationarizing the time series involved if they are $I(2)$. It may as well inform on matrix non-invertibility, on the performance of error covariances and help integrating the differenced series for correct in- and out-sample forecasting[6].

To perform updation of the states until the year 2011, the procedure utilized in the paper requires two steps: (*i*) estimation by LTI-KF of all the parameters involved with both states and observables sharing the same time length, and departing from year 1850; (*ii*) forecasting the states *s* steps ahead of the remaining years (Table 2, col. 8) by TVP, exploiting all the parameter results of step (*i*) to perform initializations. Essential to time saving and correct model identification is the choice of the most efficient parameter initialization method and the related instrumental variable among the six available BEA series. This is achieved after comparing on a grid basis the LTI first-step performance of each candidate series in terms of state covariance. The least covariance produces the desired result.

3.2. First-step Estimation of the KF State-Space Model

In State-Space (SS) discrete-time terms, after defining t a time notation of integers where $-\infty \ll t \ll \infty$, we have the following constructs applicable to the states and to the observables. Let $y_{t,k}$, $t \in [T_{y,1}, T_k]$, $k \in [1,6]$ be each of the six BEA series shown in Table 1 and graphed in Fig. 1. Their AD year of commencement is $T_{y,1} = 1850$, while their common endpoint is $T_k = 2011, \ \forall k$. Let also $j \in [1, N = 10]$ be the NOAA series order included in Table 2 (col. 1), and

[6] The ®Matlab software containing the dataset and the TVP-KF applications is available upon request from the author. It may be utilized for replication purposes.

$X_{t,j}$, $t \in [T_{j,1}, T_{j,f}]$ each characterized by a specific timespan of length ranging from $T_{j,1}$ (col. 4) to $T_{j,f}$ (col. 5). For instance, the series keynamed Hant (Hantemirov and Shiyatov, 2002) includes 4,063 observations commencing in the year $T_{j,1} = 2066$ BC and ending in year $T_{j,f} = 1996$, $j = 1$. Then, the *s* steps ahead necessary to reach the year 2011 are 13 (col. 8).

From the given time notations we have: $T_{j,1} < T_{y,1} < T_{j,f} < T_k$, $\forall j,k$, namely, every *j.th* NOAA series begins (terminates) before (beyond) the year 1850 and before the year 2011. The SS LTI model representation for the first-step estimation is given as follows

$$\begin{aligned} X_{t+1,j} &= \mathrm{A}X_{t,j} + \mathrm{B}u_{t,j} \\ y_{t,k} &= \mathrm{C}X_{t,j} + e_{t,k} \end{aligned} \tag{1}$$

where $t \in [T_{y,1}, T_{j,f}]$, and the state estimate error is $u_{t,j} \sim N(0, \mathrm{R})$, the innovation of the observable is $e_{t,k} \sim (0, \mathrm{Q})$, and $\mathrm{E}(u_{t,j}{}' e_{t,j}) = 0$, where $\mathrm{E}(.)$ is the expectational operator. The first and the second expressions of eq. (1) respectively are the state equation of motion and the observable equation. Here, the state variable is measurable, so that estimation of the underlying model may be performed by MLE if the series are normal or any other linear-quadratic optimization methods e.g. recursive subspace identification (or prediction-error) algorithms (Aoki, 1990; Ljung, 1999).

Since the model is SISO $\forall j,k$, the parameter matrices R and Q, as well as A, B and C are scalars, henceforth denoted simply as "parameters". Eq. (1) is solved for them in a recursive way over the entire time span provided. Briefly, given the assumed initial parameters at $t = 1$, eq. (1) is solved with the aim of minimizing overtime the state-covariance Riccati matrix P, i.e. to attain $\underset{t\to\infty}{Lim} \|\mathrm{P}_t\| = 0$ and to obtain a converging Kalman gain in the form of $\underset{t\to\infty}{Lim} \|\mathrm{K}_t\| = 0$, both of which are subject to the root(s) of A to be enclosed in the unit circle. Therefore, the states and the observables need stationarization if $I(1)$ originally, so that the stabilizing conditions apply, namely, $\mathrm{E}(\|\mathrm{A}\|) < 1$, $\mathrm{E}(\|\mathrm{P}_{T_{j,f}}\|) \simeq 0$, and $\mathrm{E}(\|\hat{X}_{T_{j,\infty}}\|) << \infty$. These conditions specify that the norm of A must be smaller than unity, that the expected nonlimit norm of P is close to zero and that the expected estimated value of the state(s) is below infinity. Also, controllability and observability must be ensured, although in the present context the first condition is more relevant[7].

---

[7] In standard KF (e.g. Kalman, 1960; Aoki, 1990), R and Q respectively are defined as the state and as the observable error covariance matrices. A is the state transition matrix, B the state-to-error matrix and C the state-to-observable transformation matrix. Customarily, for a state and an observable matrix respectively of size *p* and *q* $(p \geq 1; q \geq 1; p >=< q)$, and same discrete-time length *T*, we have: A, B, Q, P of size $(p \times p)$, $\mathrm{R}: (q \times q)$, $\mathrm{C}: (q \times p)$ and $\mathrm{K}: (p \times q)$. We have the state equation covariance $\mathrm{P}=X_{t+1,j}{}' X_{t+1,j}$ such that $\mathrm{P} = \mathrm{APA'} + \mathrm{B'QB}$, and $\mathrm{K}=\mathrm{APC'}(\mathrm{CPC'}+\mathrm{R})^{-1}$, where the last bracketed expression derives from the observable equation covariance $e_{t,k}{}' e_{t,k} = \mathrm{CPC'}+\mathrm{R}$. Controllability amounts to having the sequence $\{\mathrm{A}^{n-1}\mathrm{B}\} \to 0$, $n \in [1, pq]$ and observability the sequence $\{\mathrm{CA}^{n-1}\} \to 0$, $n \in [1, pq]$.

The "Kalman Triplet" that merges prediction and updating of the state(s) as well as of the Riccati matrix and of the Kalman gain in eq. (1) [8] produces the following results for $t \in [T_{y,1}, T_{j,f}]$

$$
\begin{aligned}
\hat{X}_{t+1,j} &= \mathrm{A}\hat{X}_{t,j} + \mathrm{B}u_{t,j} + \hat{\mathrm{K}}_t\left(y_{t,k} - \mathrm{C}\hat{X}_{t,j}\right) \\
\hat{\mathrm{P}}_{t+1} &= \mathrm{B'QB} + \mathrm{A}\hat{\mathrm{P}}_t\mathrm{A'} - \mathrm{KC}\hat{\mathrm{P}}_t\mathrm{A'} \\
\hat{\mathrm{K}}_t &= \mathrm{A}\hat{\mathrm{P}}_t\mathrm{C'}\left(\mathrm{R}+\mathrm{C}\hat{\mathrm{P}}_t\mathrm{C'}\right)^{-1}
\end{aligned}
\tag{2}
$$

where $X_{1,j}$ is known, and $\mathrm{P}_1 = \mathrm{B'QB}+\mathrm{AP}_1\mathrm{A'}$ and $\mathrm{K}_1 = \mathrm{AP}_1\mathrm{C'}\left(\mathrm{R}+\mathrm{CP}_1\mathrm{C'}\right)^{-1}$ are initial arbitrary values associated to the key parameters at $T_{j.1}$ [9]. The first equation represents the typical state prediction-error module (Hamilton, 1994; Ljung, 1999), while the other two are the parameter recursive matrix equations. If the stabilizing conditions apply to these equations, the process $\hat{X}_{t+1,j}$ is covariance-stationary and estimation is minimum-variance and therefore efficient.

3.3. Second-step Estimation of the KF State-Space Model

Define the steps-ahead sequence as $s_j \in [1, T_k - T_{j,f}]$, or better as $S_j = T_{j,f} + s_j$ to mark the beginning date of the recursion. Then, the SS representation of the second-step estimation with TVP-KF, to be compared with eq. (1), is the following

$$
\begin{aligned}
X_{S_j+1,j} &= \mathrm{A}X_{S_j,j} + \mathrm{B}u_{S_j,j} \\
y_{S_j,k} &= \mathrm{C}X_{t,j} + e_{S_j,k}
\end{aligned}
\tag{3}
$$

where all the parameters involved are time-varying over the s_j interval and include A_{s_j}, B_{s_j}, C_{s_j}, Q_{s_j}, R_{s_j}, P_{s_j} and K_{s_j}. Here, the state variables are unobservable except for the first observation, and initialization of the variables and parameters departs from the end results obtained from eqs. (1) and (2). Specifically, $X_{j,f} = \hat{X}_{T,j}$, $P_{j,f} = P_{T,j}$ and so on. Finally, the observable acts as a leading indicator in common econometric forecasting methods (Marcellino, 2006; Banerjee et al., 2005).

As advanced in Sect. 3.1, TVP parameter estimation keeps the operator informed about the dynamics of state updation in order to avoid explosive behavior caused by non-converging Riccati and Kalman gain matrices or non-invertibility. Moreover it enables the operator to add, if desired, noisy observations to the predicted states in order to preserve the standard deviation exhibited

---

[8] The KF distinguishes between prediction and update, respectively known in Bayesian terms as the *a priori* and the *a posteriori* state estimation. They alternate one another during the recursion: prediction produces the state estimate based on the transition matrix and the Lyapunov solution to the Riccati matrix. The state update incorporates the observed innovation while the Riccati update includes the changes occurred in the Kalman gain.

[9] Parameter initialization is no easy task in standard LTI-KF as it may rely on too restrictive and arbitrary assumptions imposed on the data and/or on the parameters themselves. Guess-based approximations, however, are frequent and in most cases inevitable and definitely shared with similar recursive methods, such as the Newton-Raphson derivative algorithm. For instance, positing P_1 and A as identity matrices respectively forces the data to be Gaussian and to follow an AR(1) process when either or both may not be so, while assigning zero values to matrix B forces the equation of motion to exhibit no error structure.

during the last period of LTI estimation. Finally, while the estimation method is identical to the previous, the initializing conditions are made to change at each forecast step and are by consequence no longer arbitrary but are instead data-based (see fn. 8). This ensures provision of consistent prior information on all parameters as no guess is involved (see fn. 8).

The analog of eq. (2) in a TVP-KF context is expressed by the following system

$$
\begin{aligned}
\hat{X}_{s+1,j} &= \mathrm{A}_t \hat{X}_{s,j} + \mathrm{B}_s u_{s,j} + \hat{\mathrm{K}}_t \left(y_{s,k} - \mathrm{C}_s \hat{X}_{s,j} \right) \\
\hat{\mathrm{P}}_{s+1} &= \mathrm{B}_s' \mathrm{Q}_s \mathrm{B}_s + \mathrm{A}_s \hat{\mathrm{P}}_s \mathrm{A}_s' - \mathrm{K}_s \mathrm{C}_s \hat{\mathrm{P}}_s \mathrm{A}_s' \\
\hat{\mathrm{K}}_s &= \mathrm{A}_s \hat{\mathrm{P}}_s \mathrm{C}_s' \left(\mathrm{R}_s + \mathrm{C}_s \hat{\mathrm{P}}_s \mathrm{C}_s' \right)^{-1}
\end{aligned} \tag{4}
$$

where the time step notation is for simplicity $s \in [1, T_s]$, for $T_s = T_k - T_{j,f}$. and where the first equation originates from the LQG controller with optimal feedback by the observable(s). Initialization of the Riccati and Kalman gain equations at each step ahead is given by the following formulas:

$$
\begin{aligned}
&\mathrm{P}_s = \mathrm{B}'\mathrm{QB} + \mathrm{APA}' - \mathrm{KCPA}', \; \mathrm{K}_s = \mathrm{AP}_s\mathrm{C}' \left(\mathrm{R} + \mathrm{CP}_s\mathrm{C}' \right)^{-1}; \text{ for } s=1 \\
&\mathrm{P}_s = \mathrm{B}_{s-1}' \mathrm{Q}_{s-1} \mathrm{B}_{s-1} + \mathrm{A}_{s-1} \mathrm{P}_{s-1} \mathrm{A}_{s-1}' - \mathrm{K}_s \mathrm{C}_{s-1} \mathrm{P}_s \mathrm{A}_{s-1}', \; \mathrm{K}_s = \mathrm{A}_{s-1} \mathrm{P}_s \mathrm{C}_{s-1}' \left(\mathrm{R}_{s-1} + \mathrm{C}_{s-1} \mathrm{P}_s \mathrm{C}_{s-1}' \right)^{-1}; \text{ for } s > 1
\end{aligned} \tag{5}
$$

where P in the first equation is the Riccati matrix evaluated at time $T_{j,f}$, $\forall j$, the end of the LTI estimation of the *j*th. state series, and similarly for the parameters A, B, C, Q and R. The subscripted parameters in the second equation are obtained from previous step estimations. By applying eqs. (3) to (5) sequentially, the parameters can be recovered and tested for the implied stabilizing conditions over the steps-ahead timespan. Some of these are identical to those of the LTI model, like those regarding the Riccati and Kalman gain matrices, i.e. $\underset{s \to T_s}{Lim} \left\| \mathrm{P}_s \right\| = 0$ and $\underset{s \to T_s}{Lim} \left\| \mathrm{K}_s \right\| = 0$, others are new like $\left\| A_s \right\| < 1$, $\left\| Q_s \right\| << \infty$, $\left\| R_s \right\| << \infty$, $\forall s \in [1, T_s]$.

4. Estimation Results of the LTI and TVP-KF SISO models

In this paper, three different initializing methods of eq. (5) are utilized and tested for the smallest state-covariance matrix in conjunction with the $k \in [1,6]$ available BEA series,. The target is to find the best performers on this account by applying a grid search at the end of the first-step LTI estimation and along the updating process. We alternatively posit three initialization methods of the Riccati matrix P: (1) the identity matrix; (2) the state measured covariance; (3) the steady state solution of the first equation in eq. (5). The last method is obtainable, given knowledge at time $T_{j,f}$ of the parameters A, B, C, Q and R, by finding the value of P that ensures the following equality

$$
0 = \mathrm{B}'\mathrm{QB} - \mathrm{P} + \mathrm{APA}' - \mathrm{APC} \left(\mathrm{R} + \mathrm{CP}_s\mathrm{C}' \right)^{-1} \mathrm{C}'\mathrm{PA}' \tag{6}
$$

which is the steady-state representation of the Riccati matrix in the first line of eq.(5). In all cases, the initialization of the Kalman gain is consequential[10].

Let the mean values of $\|\mathrm{P}\|$ for each NOAA/ BEA series combination utilized for LTI estimation be expressed as

$$m_k = \left(\sum_{j=1}^{10} \left\| \mathrm{P}_{j,k} \right\| \right) \Big/ 10, \ \forall k \in [1,6].$$

There are six of these mean norms for each of the initialization methods. The combination of the *k*th. series and the *i*th. initialization method $(i = 1,...,3)$ that achieves the minimal state covariance is found by grid search to be HADCRUT3vNH with $i = 3$[11]. The same approach is utilized for TVP estimation with identical end results which are shown in Table 5, where the real number therein are the step-by-step means of the NOAA series for each BEA series, sequentially exhibited by initialization method:

$$m_s = \left(\sum_{s=1}^{s_j} \left\| \mathrm{P}_{j,s,k} \right\| \right) \Big/ s_j, \ \forall j \in [1,10], \forall s_j \in \left[1, T_k - T_{j,f}\right] \text{ and } \forall k \in [1,6].$$

Also the series means are included, and all results confirm that use of HADCRUT3vNH with the third initialization method is optimal (box 3, col. 5). By consequence, this prefered combination of instrumental variable and initializing method is adopted to perform all the updatings of the NOAA series. Noisy data simulating the standard deviation of the latest first-differenced original observations of each series is added to the forecasted trends, as advanced in Sect. 3.3. Therefore, multiple replications of the updation process of each NOAA series by TVP-KF may produce different forecasted values proportional to the standard deviation.[12]. The implied volatility indexes, however, are found to stay substantially below those reported in Table 3 (col. 5) and to average .502, with a maximum of Hant's being 3.36 and a minimum of Tand being .012.

The averages of 1,000 Gaussian noise-added Monte Carlo replications of each NOAA series are produced for the updatings. The graphical and the quantitative mean results are exhibited in Fig.2 and Table 6, respectively. Graphically, the updates of most of the series appear no more than blips on the right-hand side of the red-marked line that splits them from the original data, and reveal little crucial by simple eyeballing. Quantitatively, instead, they shed much light on the millennial-scale analysis regarding the "hockey stick" hypothesis. Four non-neighboring local maxima,

---

[10] The first two initializations are arbitrary and equivalent to those that may be imposed at $T_{j,1}$ (see fn. 8). The last initialization is based on prior information of the estimated parameters and may produce interesting results if they are stabilizing because also the ensuing P matrix will be stable. The solution of P obtains by solving the nonlinear differential eq.(6) at its steady state.

[11] The first two methods produce $m_k = 1$ and $m_k = .358$ for all BEA series, while for the third method the following is obtained: $m_k = \{0.0042,\ 0.0072,\ 0.0033,\ 0.0061,\ 0.0736,\ 0.0340\}$, $\forall k$. Clearly the latter result is prefered on magnitude grounds, and within the sequence, the third value associated to the third BEA series is the smallest.

[12] The amount of first-differenced observations utilized for extracting the standard deviation utilized in noisy simulations is set to be $d_j \in \left[T_{j,f} - s_j, T_{j,f}\right]$, $\forall j$, i.e. the last observations of the original data, quantitatively equal to the steps-ahead forecasting time span of each NOAA series (Table 2, col. 8).

separated by a minimal distance of 150 years, are identified for each fully updated series[13]. Their achievement dates and values are sequentially reported (Table 6, cols. 4-7, and 8-13) together with the ratio of the achieved value of the first local maximum, which is also the global maximum (col. 8), evaluated with respect to the other maxima (cols. 14-16). Many of these are very close one another so that, in a noisy environment (von Storch et al., 2004; Brohan et al., 2006; McIntyre and McKitrick, 2009) the primacy might be reversed: in other words, the first local maximum may become second or third in order of magnitude due to data replications, although several climatologists may not agree on this occurrence (Mann et al., 2009b). As easily seen, only two series – Mann, and Crow – exhibit a sizable jump in the ratio that compares the first to the second achieved local maxima (col. 14), and even more so further on (cols. 15-16). Similar, albeit not so dramatic, are the jumps in D'Arrigo and maybe Moberg. The first two series place the highest achieved proxy temperatures in the year 2009, while the other two in the years 1943 and 1105, respectively.

In order to dissipate noisy-environment uncertainties on the local/global maximum achieved dates and values exhibited in Table 6, the same 1,000 Gaussian noise-added Monte Carlo replications of each NOAA series have been tested for the probabilities with which such maxima occur. Table 7 produces this outcome by reporting the ranked years of maxima and their sample probabilities, excluding those close to zero[14]. Three series (Mann, Mann1 and Crow) unmistakably espouse the "hockey stick" hypothesis by putting the maximum achieved temperatures in the years striding the 20th and the 21th centuries. One series (D'Arrigo) goes fifty-fifty between the RWP and the MWP. All of the other six series (Hant, Salz, Tand, Esper, Moberg and Moore) put heavy probability weights on the MWP and even somewhere else in the more or less distant past. For these series, therefore, the RWP never scores more than one third of the probabilities.

5. Conclusion

Several climatologists and the IPCC have since long maintained that the RWP is an unprecedented phenomenon in the climatic history of the Earth by featuring the "hockey stick" hypothesis and the associated anthropogenic origin. This purported evidence is put to test by utilizing a select batch of ten millennial-scale climate proxies, included in the NOAA 92 PCN dataset, and updated to the year 2011 by means of a TVP-KF model for state prediction. The observable utilized therein is the HADCRUT3vNH series of instrumental temperature anomalies available since the year 1850.

Out of ten series, only three significantly do not refute the hypothesis, while the others point to different maximum temperature dates, mostly included in the MWP. By consequence, from an outsider's viewpoint, the scenario mostly favorable to the "hockey stick" hypothesis would render both warming periods on the same footing (e.g. Baliunas and Soon, 2003) given Gaussian noise,

---

[13] Local non-neighboring maxima (and minima) may be identified by splitting the millennial series into equally spaced subperiods or by other procedures, e.g. moving averages or golden section. Unreported tries of shorter (100 years) or longer (200 years) gaps produce very similar results. The selected length of 150 years also fits the maximal length of the RWP thereby adequately tracing a dividing line with the previous climate epochs like the MWP and the LIA.

[14] The results shown in Table 7 are obtained as follows: for each series and for each simulation the four largest non-neighboring values and associated dates (years) are computed. Then the dates are stored in matrix $D:(1{,}000\times 4)$. The relative frequencies of each date there included are then evaluated and posted as ranked probabilities, labeled P in the table and tallying unity by column. The approximation in the percentage shares is due to the use of date integers.

contrary to the claims of the IPCC in the Fourth Assessment Report (2007) and of some authors (Jones et al., 2001; D'Arrigo et al., 2006; Mann et al., 2009a)[15]. The mostly unfavorable scenario would instead require shedding further light on the data collection and processing executed by the authors of the claim, thereby justifying the validity of I. Jolliffe's trenchant comment at Tamino appeared on the web: "I am by no means a climate change denier. My strong impressive is that the evidence rests on much more than the hockey stick. It therefore seems crazy that the … hockey stick has been given such prominence and that a group of influential climate scientists have doggedly defended a piece of dubious statistics".

Data Appendix

Two datasets are available: NOAA and BEA. The first includes ten selected series from the NOAA Paleoclimatology Reconstructions Network including 92 high-resolution temperature records over the past 2+ millennia. The keynames reported in the Tables are subsequently associated to the respective bibliographical source. BEA includes six out of nine series.

i) NOAA:

1) Hant (Hantemirov and Shiyatov, 2002): Yamal Peninsula Multimillennial Summer Temperature Reconstruction

2) Salz (Salzer and Kipfmueller, 2005): Southern Colorado Plateau Temperature and Precipitation Reconstructions

3) Tand (Tand et al., 2003): Shihua Cave, Beijing Stalagmite Temperature Reconstruction

4) Mann (Mann et al., 2008): 2,000 Year Hemispheric and Global Surface Temperature Reconstructions: Global: Land and Ocean: Error-In-Variables Method

5) Mann1 (Mann et al., 1999): Northern Hemisphere Temperatures during the Past Millennium

6) Crow (Crowley, 2000): Northern Hemisphere Temperature Reconstruction: with instrumental records after 1860

7) Esper (Esper et al., 2002): Northern Hemisphere Extratropical Temperature Reconstruction

8) D'Arrigo (D'Arrigo et al., 2006): Northern Hemisphere Tree-Ring-Based Temperature Reconstruction: Regional Curve Standardization

9) Moberg (Moberg et al., 2005): 2,000-Year Northern Hemisphere Temperature Reconstruction

10) Moore (Moore et al., 2001): Baffin Island 1250 Year Summer Temperature Reconstruction

[15] The first authors declare that: "Average temperatures during the last three decades were likely the warmest of the last millennium, about 0.2C warmer than during warm periods in the 11th and 12th centuries", while the others declare that their data: "reconstruction suggests that MWP temperatures were nearly 0.7C cooler than in the late twentieth century, with an amplitude difference of 1.14C from the coldest (1600-1609) to warmest (1937-1946) decades". Finally, Mann et al. declare that: "The Medieval period is found to display warmth that matches or exceeds that of the past decade in some regions, but which falls well below recent levels globally".

ii) BEA: HADCRUT3, HADCRUT3v and HADSST2 all updated to 2011 and containing both global (GL) and Northern Hemisphere (NH) records. HADSST2 is sea surface temperature anomalies (Rayner et al., 2006), HADCRUT3 is combined land and marine sea surface temperature (SST) anomalies from HADSST2 (Brohan et al., 2006), HADCRUT3v is the variance adjusted version of HADCRUT3.

References

Abdussamatov H. (2004) *About the Long-Term Coordinated Variations of the Activity, Radius, Total Irradiance of the Sun and the Earth's Climate*, International Astronomical Union, DOI: 10.1017/S1743921304006775, 541-542.

Alanko-Huotari, K., I.G. Usoskin, K. Mursula, and Kovaltsov G.A. (2006) *Global Heliospheric Parameters and Cosmic Ray Modulation: an Empirical Relation for the Last Decades*, Solar Physics, 238, 391-404.

Anderson B.D.O. and Moore J.B. (2005) *Optimal Filtering*, Dover Publications.

Aoki M. (1990) *State space modeling of time series*, Springer-Verlag.

Appenzeller C., Stocker T.F. and Anktin M. (1998) *North Atlantic Oscillation Dynamics Recorded in Greenland Ice Cores*, Science, 282, 446-449.

Baliunas S. and Soon W. (2003) *Lessons and Limits of Climate History: Was the 20th. Century Climate Unusual?*, The George C. Marshall Institute, Washington D.C.

Banerjee A., Marcellino M. and Masten I. (2005) *Leading Indicators for Euro-area Inflation and GDP Growth*, Oxford Bulletin of Economics & Statistics, 67, 785-813.

Bard E. and Frank M. (2006) *Climate Change and Solar Variability: What's new Under the Sun?*, Earth and Planetary Science Letters, 248, 1-14.

Bradley R.S. (1999) *Paleoclimatology: Reconstructing Climates of the Quaternary*, Harcourt Academic Press, San Diego, CA.

Bradley R.S., Briffa K.R., Crowley T. J., Hughes M. K., Jones P.D. and Mann M.E. (2001) *Scope of Medieval Warming*, Science, 292, 2011-2012.

Briffa K.R., Jones P.D. and Schweingruber F.H. (1994) *Summer Temperatures across Northern North America: Regional Reconstructions from 1760 Using Tree-ring Densities*, Journal of Geophysical Research, 99, 835-25.

Briffa, K.R., Osborn T. J., Schweingruber F. H., Harris I. C., Jones P. D., Shiyatov S. G., and Vaganov E. A. (2001) *Low-frequency Temperature Variations from a Northern Tree-ring Density Network*, Journal of Geophysical Research, 106, 2929-2941.

Briffa KR, Osborn T. J. and Schweingruber F.H (2003) *Large-scale Temperature Inferences from Tree Rings: a Review*, Global and Planetary Change 40, 11-26, DOI:10.1016/S0921-8181(03)00095-X.

Brohan P., Kennedy J.J., Harris I., Tett S.F.B. and Jones P.D. (2006*) Uncertainty Estimates in Regional and Global Observed Temperature Changes: a new Dataset from 1850*, Geophysical Research, 111, DOI:10.1029/2005JD006548.

Bürger G., (2007) *Comment on the Spatial Extent of 20th-Century Warmth in the Context of the Past 1200 Years*, Science, 316/5833, 1844.

Choudry T. and Wu H. (2008) *Forecasting Ability of GARCH vs Kalman Filter Method: Evidence from Daily UK Time-Varying Beta*, Journal of Forecasting, 27, 670-689.

Crowley, T.J. and. North G.R (1991) *Paleoclimatology*, Oxford University Press.

Crowley, T.J. (2000) *Causes of Climate Change Over the Past 1000 Years*, Science, 289, 270-277.

Crowley, T. J. and T. Lowery, 2000, *How Warm Was the Medieval Warm Period?* Ambio*,* 29, 51-54.

D'Arrigo, R., Wilson R., and Jacoby G. (2006) *On the Long-Term Context for Late Twentieth Century Warming*, Journal of Geophysical Research, 111, D03103, DOI: 10.1029/2005JD006352.

Dickey, D.A. and Fuller W.A. (1979) *Distribution of the Estimators for Autoregressive Time Series with a Unit Root*, Journal of the American Statistical Association, 74, 427–431.

Engle R. and Granger C.W. (1987) *Cointegration and Error Correction: Representation, Estimate, and Testing*, Econometrica*,* 55, 251–276.

Esper, J., Cook E.R. and Schweingruber F.H. (2002) *Low-Frequency Signals in Long Tree-Ring Chronologies for Reconstructing Past Temperature Variability*, Science, 295, 2250-2253.

Esper J. and Frank D. (2009) *The IPCC on a Heterogeneous Medieval Warm Period*, Climatic Change, 94, 267–273.

Evans M.N., Kaplan A. and Cane M.A. (2002) *Pacific Sea Surface Temperature Field Reconstruction from Coral δ18O Data Using Reduced Space Objective Analysis*, Paleoceanography, 17, DOI:10.1029/2000PA000590.

Folland C.K., Karl T.R., Christy J.R., Clarke R.A., Gruza G.V., Jouzel J., Mann M.E., Oerlemans J., Salinger M.J. and Wang S.W. (2001) *Observed Climate Variability and Change, in Climate Change 2001: The Scientific Basis,* Houghton J.T. et al. (eds.), Cambridge Univ. Press, Cambridge, 99-181.

Fouka P., Fröhlich C., Spruit H. and Wigley T.M. (2006) *Variations in Solar Luminosity and their Effect on the Earth's Climate*, Nature, 443, 161-166.

Fritts H.C., Blasing T.J., Hayden B.P. and Kutzbach J.E. (1971) *Multivariate Techniques for Specifying Tree-growth and Climate Relationships and for Reconstructing Anomalies in Paleoclimate*, Journal of Applied Meteorology, 10, 845-864.

Fritts, H.C. (1991) *Reconstructing Large-scale Climatic Patterns from Tree-Ring Data*, The University of Arizona Press.

Graham N.E., Ammann C.M., Fleitmann D., Cobb K.M., and Luterbacher J. (2010) *Support for Global Climate Reorganization during the "Medieval Climate Anomaly"*, Climate Dynamics, DOI: 10.1007/s00382-010-0914-z.

Gray W.M., Sheaffer J.D. and Landsea C.W. (1997) *Climate Trends Associated with Multidecadal Variability of Atlantic Hurricane Activity*, in Diaz H.F. and Pulwarty R.S. eds*., Hurricanes: Climate and Socioeconomic Impacts*, Springer-Verlag, New York, N.Y., 15-53.

Grimble M.J. (2006) *Robust Industrial Control Systems: Optimal Design Approach for Polynomial Systems*, Wiley.

Hamilton J.D. (1994) *Time Series Analysis*, Princeton University Press.

Hantemirov, R.M. and Shiyatov S.G. (2002) *A Continuous Multimillennial Ring-width Chronology in Yamal, Northwestern Siberia*, Holocene 12, 717-726.

Hendy**,** E. J., Gagan M. K., Alibert C. A., McCulloch M. T., Lough J. M. and Isdale P.J. (2002) *Abrupt Decrease in Tropical Pacific Sea Surface Salinity at End of Little Ice Age*, Science, 295, 1511-154.

IPCC (2001) Third Assessment Report, (2007) Fourth Assessment Report.

Johansen S. (1988) *Statistical Analysis of Cointegration Vectors*, Journal of Economic Dynamics and Control, 12, 231-254.

Johansen S. (1991) *Estimation and Hypothesis Testing of Cointegration Vectors in Gaussian Vector Autoregressive Models*, Econometrica, 59, 1551-1580.

Jones P.D., Osborn T.J., and Briffa K.R. (2001) *The Evolution of Climate Over the Last Millennium*, Science, 292, 662-667.

Kalman R.E. (1960) *A New Approach to Linear Filtering and Prediction Problems*, Transactions of the ASME – Journal of Basic Engineering, 82, 35-45.

Loso, M.G. (2008) *Summer Temperatures during the Medieval Warm Period and Little Ice Age Inferred from Varved Proglacial Lake Sediments in Southern Alaska*, Journal of Paleolimnology 41, 117-128, DOI: 10.1007/s10933-008-9264-9.

Ljung L. (1999) *System Identification. Theory For the User,* Prentice Hall.

Mann M.E., Bradley R.S. and Hughes M.K. (1998) *Global-scale Temperature Patterns and Climate Forcing Over the Past Six Centuries*, Nature, 392, 779-787.

Mann M.E., Bradley R.S. and Hughes M.K. (1999) *Northern Hemisphere Temperature During the Past Millennium: Inferences, Uncertainties and Limitations*, Geophysical Research Letters, 26, 759-762.

Mann M.E., Zhang Z., Hughes M.K., Bradley R.S., Miller S.K., Rutherford S., and Ni F. (2008) *Proxy-based Reconstructions of Hemispheric and Global Surface Temperature Variations Over the Past Two Millennia*, Proceedings of the National Academy of Sciences, 105, 13252-13257.

Mann M.E., Zhang Z., Rutherford S., Bradley R.S., Hughes M.K., Shindell D., Ammann C., Faluvegi G., and Ni F. (2009) *Global Signatures and Dynamical Origins of the Little Ice Age and Medieval Climate Anomaly*, Science, 326, 1256-1260.

Mann M.E., Bradley R.S. and Hughes M.K. (2009b) *Reply to McIntyre and McKitrick: Proxy-based Temperature Reconstructions are Robust*, Letter in Proceedings of the National Academy of Sciences, 106, E11.

Marcellino M. (2006) *Leading Indicators*, in: Elliott, G., Granger, C.W.J., Timmermann, A. (Eds.), Handbook of Economic Forecasting. Elsevier, Amsterdam.

McIntyre S. and McKitrick R. (2005) *The M&M Critique of the MBH98 Northern Hemisphere Climate Index: Update and Implications***,** Energy and Environment, 16, 69-100.

McIntyre S. and McKitrick R. (2009) *Proxy Inconsistency and Other Problems in Millennial Paleoclimate Reconstructions*, Letter in Proceedings of the National Academy of Sciences, 106, E10.

Moberg, A., Sonechkin D.M., Holmgren K., Datsenko N.M. and Karlén W. (2005) *Highly Variable Northern Hemisphere Temperatures Reconstructed from Low- and High-resolution Proxy Data*, Nature 433:613-617.

Montford A.W. (2010) *The Hockey Stick Illusion*, *Climategate and the Corruption of Science*, Stacey International, London UK.

Moore, J.J., Hughen K.A., Miller G.H. and Overpeck J.T. (2001) *Little Ice Age Recorded in Summer Temperatures from Varved Sediments of Donard Lake, Baffin Island, Canada*, Journal of Paleolimnology 25, 503-517, DOI: 10.1023/A:1011181301514.

National Research Council (2006) *Surface Temperature Reconstructions for the last 2,000 Years*, Board on Atmospheric Sciences and Climate, Division on Earth and Life Studies, The National Academies Press, Washington, D.C.

O'Brien, S.R., Mayewski P.A, Meeker L.D., Meese D.A., Twickler M.S. and Whitlow S.I. (1995) *Complexity of Holocene Climate as Reconstructed from a Greenland Ice Core*, Science, 270, 1962-1964.

Rayner, N.A., Brohan P., Parker D.E., Folland C.K., Kennedy J.J., Vanicek M., Ansell T. and Tett S.F.B. (2006) *Improved Analyses of Changes and Uncertainties in Marine Temperature Measured in Situ Since the Mid-nineteenth Century: the HadSST2 Dataset.* J. Climate*,* 19, 446-469.

Rutherford S., Mann M.E., Osborn T.J., Bradley R.S., Briffa, K.R., Hughes M.K., and Jones, P.D. (2005) *Proxy-based Northern Hemisphere Surface Temperature Reconstructions: Sensitivity to Method, Predictor Network, Target Season, and Target Domain*, Journal of Climate, 18, 2308-2329.

Salzer, M.W. and Kipfmueller K.F. (2005) *Reconstructed Temperature and Precipitation on a Millennial Timescale from Tree-Rings in the Southern Colorado Plateau, U.S.A.*, Climatic Change 70, 465-487, DOI: 10.1007/s10584-005-5922-3

Shaviv N. (2005) *On Climate Response to Changes in the Cosmic Ray Flux and Radiative Budge*t, Journal of Geophysical Research, 110, 1-15.

Shindell D.T., Schmidt G.A., Mann E.M. and Faluvegi G. (2004) *Dynamic Winter Climate Response to Large Tropical Volcanic Eruptions since 1600*, Journal of Geophysical Research, 109, D05104, 1-12.

Svensmark H. and Frijs-Christensen E. (2007) *Reply to Lockwood and Fröhlich. The Persistent Role of the Sun in Climate Forcing*, Danish National Space Center Scientific Report 3.

Tand, M., Liu T.S., Hou J., Qin X., Zhang H. and Li T. (2003) *Cyclic Rapid Warming on Cntennial-scale Revealed by a 2650-year Stalagmite Record of Warm Season Temperature*, Geophysical Research Letters 30, 1617, DOI: 10.1029/2003GL017352.

Trouet, V., Esper J., Graham N.E., Baker A., Scourse J.D. and Frank D.C. (2009) *Persistent Positive North Atlantic Oscillation Mode Dominated the Medieval Climate Anomaly*, Science, 324, 78-80.

Usoskin I.G., Mursula K., Solanki S., Schüssler M. and Alanko-Huotari K. (2004a) *Reconstruction of Solar Activity for the Last Millennium using* ^{10}Be *Data*, Astronomy and Astrophysics, 413, 745-751.

Usoskin I.G., Mursula K., Solanki S., Schüssler M. and Alanko-Huotari K. (2004b) *Millennium-Scale Sunspot Number Reconstruction: Evidence for an Unusually Active Sun since the 1940s*, Physical Review Letters, 91, 211101:1-4.

Usoskin I.G., Solanki S.K. and Korte M. (2006) *Solar Activity Reconstructed over the Last 7000 years: The Influence of Geomagnetic Field Changes*, Geophysical Research Letters, 33, L08103, 1-4.

von Storch H., Zorita E., Jones J.M., Dimitriev Y., González-Rouco F. and Tett S.F.B. (2004) *Reconstructing Past Climate from Noisy Data*, Science, 306, 679-682.

Wahl, E.R., Anderson D.M., Bauer B.A., Buckner R., Gille E.P., Gross W.S., Hartman M., and Shah A. (2010) *An Archive of High-resolution Temperature Reconstructions over the past 2+ Millennia*, Geochem. Geophys. Geosyst. G^3, 11, Q01001, DOI: 10.1029/2009GC002817.

Wegman E.J., Scott D.W., and Said Y.H. (2006) *Ad Hoc Committee Report on the "Hockey Stick" Global Climate Reconstruction*, U.S. House Committee on Energy and Commerce, Washington, D.C.

Table 1.
Descriptive statistics of BEA series and ADF test statistics for stationarity.

BEA series	1. Mean	2. Standard deviation	3. Minimum level year	4. Maximum level year	5. ADF Level *t*-test statistic	6. ADF level *p*-value	7. ADF first-difference *t*-test statistic	8. ADF first difference *p*-value
Hadcrut3NH	-0.111	0.288	1862	2005	-0.836	0.344	-9.086	0.001
Hadcrut3GL	-0.160	0.265	1911	1998	-0.963	0.298	-8.634	0.001
Hadcrut3vNH	-0.112	0.283	1862	2005	-0.765	0.370	-8.786	0.001
Hadcrut3vGL	-0.162	0.262	1911	1998	-1.664	0.091	-8.173	0.001
Hadsst2NH	-0.115	0.245	1910	2004	-1.626	0.098	-9.696	0.001
Hadsst2GL	-0.168	0.242	1910	1998	-1.273	0.187	-10.093	0.001

Table 2.
NOAA original series timelines.

1. Series order	2. Series keyname	3. Total length of series (years)	4. AD/BC year of series beginning	5. AD year of end of series	6. Number of observations corresponding to year 1850	7. Total number of years. available for BEA estimation	8. Number of steps ahead (*s*) required for updating until 2011
1	Hant	4063	-2066	1996	3917	147	15
2	Salz	2248	-251	1996	2102	147	15
3	Tand	2651	-665	1985	2516	136	26
4	Mann	1507	500	2006	1351	157	5
5	Mann1	981	1000	1980	851	131	31
6	Crow	994	1000	1993	851	144	18
7	Esper	1162	831	1992	1020	143	19
8	D'Arrigo	1283	713	1995	1138	146	16
9	Moberg	1979	1	1979	1850	130	32
10	Moore	1241	752	1992	1099	143	19

Table 3.
NOAA original series basic statistics and ADF test statistics for stationarity.

1. Series order	2. Series keyname	3. Mean	4. Standard deviation	5. Volatility index	6. ADF *t*-test statistic	7. ADF *p*-value
1	Hant	0.000	1.089	3538.597	-47.600	0.001
2	Salz	15.256	0.479	0.031	-0.345	0.526
3	Tand	22.705	0.783	0.034	-0.161	0.593
4	Mann	-0.262	0.197	0.752	-1.178	0.220
5	Mann1	-0.112	0.131	1.169	-3.746	0.001
6	Crow	-0.071	0.110	1.544	-1.203	0.211
7	Esper	0.998	0.138	0.139	-0.401	0.505
8	D'Arrigo	-0.385	0.207	0.538	-2.414	0.015
9	Moberg	-0.354	0.220	0.622	-3.397	0.001
10	Moore	2.917	0.893	0.306	-1.175	0.222

Table 4.
Engle-Granger (EG) and Johansen (JO) cointegration tests between the BEA series HADCRUT3NH and the NOAA original series.

1. Series order	2. Series keyname	3. EG *t*-test statistic	4. EG *p*-value	5. JO trace test statistic for zero cointegrating vectors	6. JO trace test statistic for zero against one cointegrating vectors
1	Hant	-149.252	0.001	73.380	20.381
2	Salz	-47.930	0.001	38.742	11.897
3	Tand	-60.945	0.001	40.404	18.445
4	Mann	-105.133	0.001	147.992	26.138
5	Mann1	-85.734	0.001	49.347	18.180
6	Crow	-39.419	0.003	48.210	0.958
7	Esper	-84.359	0.001	45.452	21.215
8	D'Arrigo	-54.594	0.001	36.458	12.444
9	Moberg	-23.004	0.085	66.189	17.443
10	Moore	-86.619	0.001	55.095	22.210

Table 5.

Grid of *s* steps-ahead Riccati matrix (P) norms of NOAA series as a function of different BEA series with three different initialization methods of P.

BEA/NOAA series		1. Hadcrut3 NH	2. Hadcrut3 GL	3. Hadcrut3v NH	4. Hadcrut3 vGL	5. Hadsst2 NH	6. Hadsst2 GL
Method 1: P identity matrix							
1	2	3	4	5	6	7	8
1	Hant	0.177	0.546	0.074	0.439	1.378	1.987
2	Salz	0.010	0.035	0.004	0.027	0.095	0.200
3	Tand	0.005	0.043	0.001	0.033	0.325	0.140
4	Mann	0.000	0.000	0.000	0.000	0.001	0.001
5	Mann1	0.001	0.048	0.000	0.038	2.068	0.111
6	Crow	0.001	0.001	0.001	0.001	0.002	0.001
7	Esper	0.004	0.010	0.003	0.009	0.027	0.057
8	D'Arrigo	0.003	0.009	0.002	0.008	0.079	0.025
9	Moberg	0.001	0.002	0.001	0.002	0.010	0.006
10	Moore	0.064	0.195	0.016	0.106	0.650	1.479
11	Mean	0.266	0.890	0.102	0.663	4.634	4.007
Method 2: P state measured covariance							
1	2	3	4	5	6	7	8
1	Hant	0.115	0.360	0.048	0.288	1.118	1.423
2	Salz	0.018	0.060	0.007	0.046	0.281	0.281
3	Tand	0.008	0.072	0.001	0.054	0.441	0.216
4	Mann	0.002	0.004	0.001	0.003	0.016	0.010
5	Mann1	0.002	0.051	0.001	0.040	2.379	0.119
6	Crow	0.006	0.013	0.004	0.012	0.013	0.009
7	Esper	0.005	0.015	0.003	0.013	0.115	0.077
8	D'Arrigo	0.006	0.018	0.003	0.015	0.110	0.049
9	Moberg	0.001	0.007	0.001	0.005	0.020	0.014
10	Moore	0.059	0.180	0.015	0.098	0.669	1.399
11	Mean	0.221	0.780	0.083	0.574	5.161	3.596

Method 3: P steady state solution							
1	2	3	4	5	6	7	8
1	Hant	0.005	0.028	0.002	0.020	0.373	0.448
2	Salz	0.000	0.002	0.000	0.001	0.101	0.059
3	Tand	0.000	0.006	0.000	0.006	0.248	0.029
4	Mann	0.000	0.000	0.000	0.000	0.000	0.000
5	Mann1	0.001	0.044	0.000	0.036	1.677	0.104
6	Crow	0.001	0.001	0.001	0.001	0.001	0.001
7	Esper	0.004	0.008	0.003	0.008	0.019	0.050
8	D'Arrigo	0.000	0.002	0.000	0.002	0.049	0.004
9	Moberg	0.000	0.000	0.001	0.000	0.003	0.001
10	Moore	0.002	0.007	0.001	0.003	0.677	0.507
11	Mean	0.013	0.097	0.008	0.077	3.148	1.201

Table 6.
Updated NOOA series timelines, four maximum achieved dates, values and ratios.
Results obtained from averaging 1,000 Monte Carlo replications of each series.

1. Series order	2. Series keyname	3. Total number of observations (years)	4. First achieved maximum date	5. Second achieved maximum date	6. Third achieved maximum date	7. Fourth achieved maximum date	8. First achieved maximum value
1	Hant	4078	994	554	791	370	3.500
2	Salz	2263	404	1981	1786	-164	17.090
3	Tand	2677	32	1964	715	1100	24.757
4	Mann	1512	2009	968	587	786	0.485
5	Mann1	1012	1944	1249	1086	1772	0.278
6	Crow	1012	2009	1087	1304	1515	0.581
7	Esper	1181	995	1958	842	1327	1.529
8	D'Arrigo	1299	1943	895	1434	1763	0.370
9	Moberg	2011	1105	896	1940	704	0.372
10	Moore	1260	1468	1300	1907	1095	7.093
9. Series order	Mean	11. Second achieved maximum value	12. Third achieved maximum value	13. Fourth achieved maximum value	14. Ratio of 8 to 11	15. Ratio of 8 to 12	16. Ratio of 8 to 13
1	Hant	3.130	3.130	3.070	1.118	1.118	1.140
2	Salz	17.040	16.990	16.900	1.003	1.006	1.011
3	Tand	24.402	24.257	24.248	1.015	1.021	1.021
4	Mann	0.163	0.112	0.008	2.969	4.323	60.128
5	Mann1	0.272	0.190	0.122	1.024	1.465	2.281
6	Crow	0.130	0.040	-0.020	4.469	14.525	-29.050
7	Esper	1.338	1.249	1.199	1.143	1.224	1.275
8	D'Arrigo	0.280	0.080	0.080	1.321	4.625	4.625
9	Moberg	0.357	0.248	0.051	1.042	1.502	7.360
10	Moore	6.611	6.249	6.201	1.073	1.135	1.144

Table 7.
Updated NOAA series. Years of achieved local maxima ranked by probability.
Results from 1,000 Monte Carlo replications of each series and for subperiods of 150 years.

Rank/ Series	1. Hant		2. Salz		3. Tand		4. Mann		5. Mann1		6. Crow		7. Esper		8. D'Arrigo		9. Moberg		10. Moore	
Rank	Y	P	Y	P	Y	P	Y	P	Y	P	Y	P	Y	P	Y	P	Y	P	Y	P
1	994	0.33	1786	0.33	715	0.33	2009	0.26	1944	0.85	2009	0.25	995	0.33	1943	0.50	1105	0.50	1907	0.33
2	554	0.33	404	0.33	32	0.33	2007	0.25	2004	0.02	2010	0.17	842	0.33	895	0.50	896	0.23	1468	0.33
3	791	0.13	2005	0.04	1964	0.14	2010	0.23	1996	0.02	2007	0.12	2008	0.03			2004	0.03	1300	0.33
4	2010	0.03	2002	0.03	1998	0.02	2008	0.20	1983	0.02	2008	0.09	1993	0.03			2007	0.02		
5	2002	0.02	2003	0.03	1988	0.02	2006	0.06	1981	0.02	2004	0.09	1995	0.02			1994	0.02		
6	2009	0.02	2001	0.03	1999	0.01			2006	0.01	2005	0.07	1994	0.02			2002	0.02		
7	2003	0.02	2000	0.03	1996	0.01			2005	0.01	2003	0.07	2007	0.02			1999	0.02		
8	2008	0.02	2007	0.02	1986	0.01			1999	0.01	2001	0.05	2006	0.02			1998	0.02		
9	2001	0.02	1999	0.02	2010	0.01			1993	0.01	2006	0.04	2001	0.02			1990	0.02		
10	1999	0.02	2010	0.02	2008	0.01			1992	0.01	1996	0.02	1998	0.02			2008	0.01		
11	1998	0.01	2008	0.02	2005	0.01			1988	0.01	2002	0.01	1996	0.02			2006	0.01		
12	1997	0.01	2004	0.02	2004	0.01			1987	0.01	1998	0.01	2009	0.02			2000	0.01		
13	2006	0.01	2009	0.02	2002	0.01					1997	0.01	2005	0.02			1997	0.01		
14	2005	0.01	1997	0.02	2000	0.01							2004	0.02			1996	0.01		
15	2007	0.01	1981	0.02	2007	0.01							1999	0.02			1995	0.01		

Y: Year, P: Probability.

Figure 1
BEA Hadcrut3 and Hadsst2 level temperature anomaly series, 1850–2011

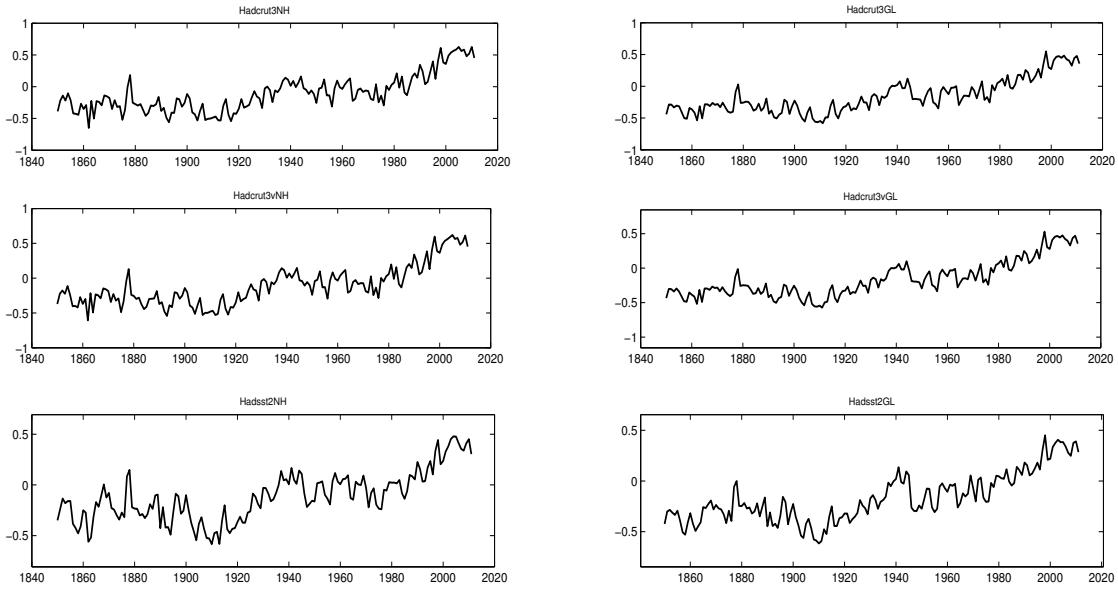

Fig. 2a.
Fully updated paleoclimate time series.

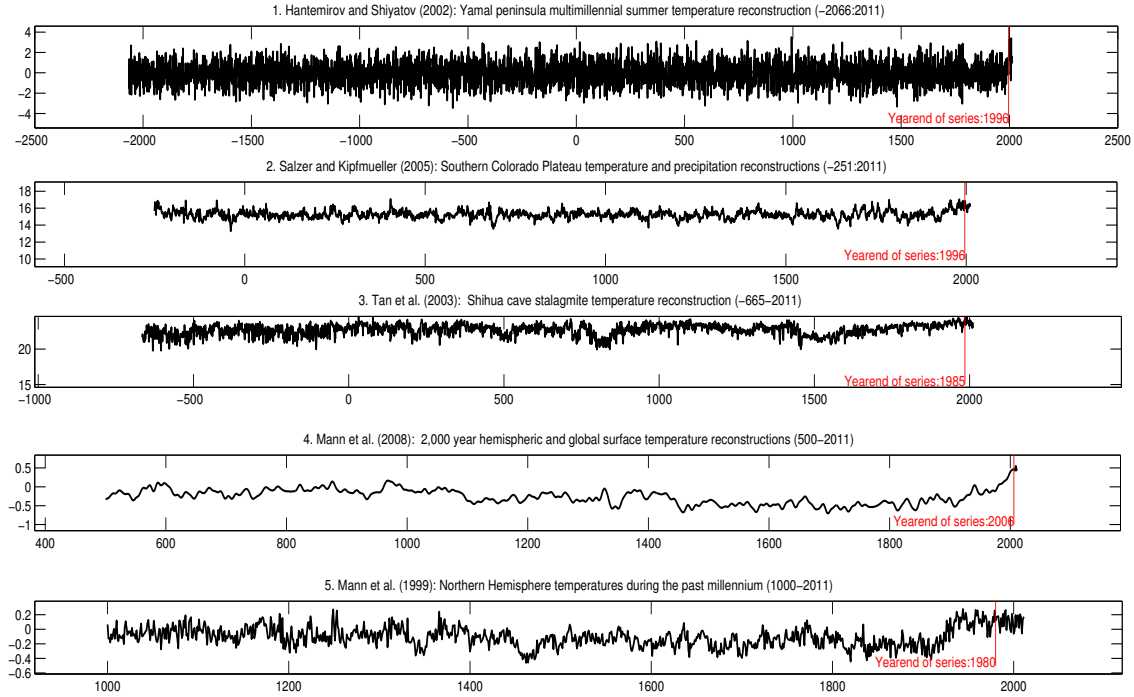
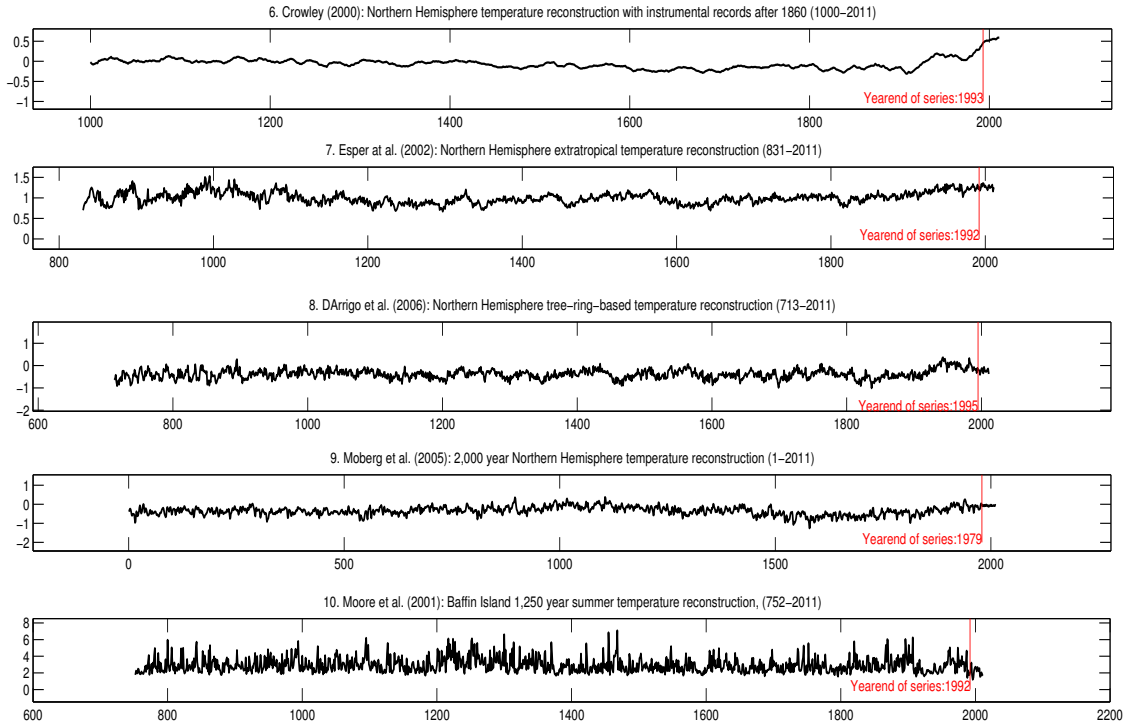
Fig. 2b.
Fully updated paleoclimate time series.